Available online at www.sciencedirect.com
SCIENCE DIRECT®
Journal of Solid State Chemistry 177 (2004) 3202–3211
JOURNAL OF SOLID STATE CHEMISTRY
http://elsevier.com/locate/jssc

Synthesis of chloroantimonates(III) with selected organic cations. X-ray studies of phase transition in ferroelectric tris(trimethylammonium) nonachlorodiantimonate(III) at 125 K

Maciej Bujak and Jacek Zaleski*

Institute of Chemistry, University of Opole, Oleska 48, Opole 45-052, Poland

Received 8 April 2004; received in revised form 18 May 2004; accepted 19 May 2004

Available online 15 July 2004

Abstract

The dependence of molar ratio of reactants on the formula, crystal structure and physicochemical properties of chloroantimonates(III) with different organic cations was studied. It was proved, that the compounds show preferences in crystallization of one product. The changes of the molar ratio of substrates lead to the corresponding changes of these components in crystallized products. The structure of ferroelectric chloroantimonate(III), $[(CH_3)_3NH]_3[Sb_2Cl_9]$, was determined at 165 and 95 K. It crystallizes in monoclinic space group *Pc*: $a = 9.9612(11)$, $b = 9.0714(8)$, $c = 15.1807(14)$ Å, $\beta = 90.086(8)^\circ$, $R_1 = 0.0202$, $wR_2 = 0.0405$ and $a = 9.9138(10)$, $b = 9.0783(7)$, $c = 15.1299(14)$ Å, $\beta = 90.026(8)^\circ$, $R_1 = 0.0163$, $wR_2 = 0.0356$ at 165 and 95 K, respectively. At both temperatures the crystal is built of polyanionic layers and trimethylammonium cations. They are bound together by the system of hydrogen bonds. The molecular motions of the organic cations are gradually frozen with decreasing temperature. At 165 K all cations are ordered. The non-structural ferro-ferroelectric phase transition at 125 K is associated with changes in the dynamics of trimethylammonium cations.

Keywords: Chloroantimonates(III); Crystal structure; Octahedral deformation; Hydrogen bonding; Ferro-ferroelectric phase transition

1. Introduction

The crystals of halogenoantimonates(III) and halogenobismuthates(III) with the general formula $R_aM_bX_c$, where R corresponds to an organic cation; M is a trivalent antimony and/or bismuth atom; X is a halogen atom (Cl, Br and/or I) and a, b, c are stoichiometric coefficients related through $c = a + 3b$, have been widely investigated due to their complex crystal chemistry and interesting physical properties connected to the different phase transitions [1–4].

Halogenoantimonates(III) and halogenobismuthates(III) may be obtained in reaction of a chosen organic substance (e.g., amine) and antimony(III) or bismuth(III) oxide in the appropriate solvent. Changes in conditions of the synthesis including the ratio of reactants, type of solvent, method of crystallization, and even the temperature, allow one to crystallize one or more products with different chemical and physical properties [5–8].

The unique crystal chemistry of these mixed organic–inorganic salts is associated with the tendency of $[MX_5]^{2-}$ square pyramids and $[MX_6]^{3-}$ octahedra to join each other through bridging halogen atoms. It results in a large number of types of anionic sublattices—isolated units, chains or layers—characteristic of each formula. The formation of specific anionic sublattices seems to be mainly determined by the countercations, but the basic properties such as charge, size and shape are usually not predictable without the structural investigations. Different in size, symmetry and ability to form hydrogen bonds organic cations together with the combination of appropriate halogen atoms provide a rich family of salts, in which above-mentioned properties, could be rationally varied. Additionally, since the structures of these crystals are partly stabilized by the hydrogen bonding system, it is

*Corresponding author. Fax: +48-77-441-0741.
E-mail address: zaleski@uni.opole.pl (J. Zaleski).

0022-4596/$ - see front matter © 2004 Elsevier Inc. All rights reserved.
doi:10.1016/j.jssc.2004.05.036

possible to influence the phase transition behavior and the geometry of coordination polyhedra by the number and geometry of the hydrogen donor sites of cations.

The nature of phase transitions in halogenoantimonates(III) and halogenobismuthates(III) is related either to a disorder of organic cations and inorganic polyhedra as well as a reorientation of organic cations and thus changing the hydrogen bonding scheme [e.g., 3,4 and references therein]. From the dielectric point of view the most important are mainly salts with relatively small alkylammonium: methyl-, dimethyl-, trimethyl- and tetramethylammonium cations. Among them from the point of view of polar properties the most interesting are crystals of the $[(CH_3)_nNH_{4-n}]_3[M_2X_9]$ ($n = 1$, 2, 3 or 4) formula with anionic sublattices built of two-dimensional $[\{M_2X_9\}_n]^{3n-}$ layers or isolated face-sharing $[M_2X_9]^{3-}$ bioctahedra as well as the $(CH_3NH_3)_5[Bi_2X_{11}]$ salts. The ferroelectric phases in these salts were, among other things, found in: $(CH_3NH_3)_3[Sb_2Br_9]$ (MABA) [9], $[(CH_3)_2NH_2]_3[Sb_2Cl_9]$ (DMACA) [10], $[(CH_3)_3NH]_3[Sb_2Cl_9]$ (TMACA) [11], and $(CH_3NH_3)_5[Bi_2Br_{11}]$ (MAPBB) [12]. The new ferroelectric crystal, 4-aminopyridinium tetrachloroantimonate(III) of the $RSbCl_4$ formula has also been recently reported by Jakubas et al. [13].

We wanted to improve our understanding of the formation of specific mixed organic–inorganic ferroic materials, the mechanisms of the phase transitions and the role, which the hydrogen bonding system plays in generation of polar properties in structures of chloroantimonates(III). Herein we describe the systematic investigations of chloroantimonates(III) with selected organic cations. We also carried out the X-ray structural studies, across the low-temperature phase transitions, reported at 203 and 125 K [3], in one of the most interesting chloroantimonate(III)—ferroelectric $[(CH_3)_3NH]_3[Sb_2Cl_9]$ crystal.

2. Experimental

2.1. Preparation and characterization of chloroantimonates(III) with organic cations

Antimony(III) chloride (for synthesis), dimethylamine (40% solution in water, for synthesis), tetramethylammonium chloride (for synthesis), ethylamine (70% solution in water, for synthesis), *N*,*N*-dimethylethylenediamine (for synthesis, all Merck-Schuchardt), methylamine (70% solution in water, Riedel-de Haën), trimethylamine (40% solution in water, Aldrich Chemical Company, Inc.), ethylenediamine hydrochloride (pure, LOBA Chemie), *N*,*N*,*N*′,*N*′-tetramethylguanidine (pure, Koch-Light Laboratories, Ltd.) and concentrated hydrochloric acid (pure p. a., POCh) were the starting materials used for the synthesis of chloroantimonates(III) with organic cations.

All single crystals were obtained using the same synthetic procedure. $SbCl_3$ (3.0–50.0 mmol) dissolved in warm ca. 6 M HCl (1.0–10.0 mL) were treated with organic substances (3.0–20.0 mmol) in the same solvent (1.0–22.0 mL). Hydrochloric acid, if necessary, was added until the precipitated substrates/products disappeared. The starting materials were used in the molar ratios varying from 0.1:1 to 10:1 (molar ratio of organic substance to antimony(III) atom). The acid solutions were allowed to slowly evaporate at room temperature until the transparent, colorless crystals were grown.

The crystals obtained in a manner stated above were characterized by the elemental analysis, determinations of melting points, densities using flotation method with a mixture of $CHCl_3$, CCl_4 and $CHBr_3$ as well as the preliminary X-ray investigations with the determination of the unit cell parameters and X-ray single-crystal studies [14–18].

2.2. X-ray measurements and structure determinations

The measurements at 165 and 95 K were performed on a Xcalibur CCD diffractometer equipped with an Oxford Cryosystems cooler. The reflections were measured using the φ- and ω-scan techniques with $\Delta\omega = 1.0^\circ$ and $\Delta t = 10$ s. The unit cell parameters were obtained from a least squares refinement of 7552 and 7496 reflections at 165 and 95 K, respectively.

Both structures were solved by the Patterson method. All data were subjected to Lorentz, polarization and empirical absorption corrections based on the symmetry-equivalent reflections [19].

All hydrogen atoms were located in subsequent maps, refined using a riding model and constrained to a distance of 0.96 and 0.90 Å for $-CH_3$ and $-NH^+$ groups, respectively. The hydrogen atoms were allowed to ride on the C and N atoms and to rotate around the neighboring C–N bonds. Their displacement parameters were taken with coefficients 1.5 and 1.2 times larger than the respective parameters of the methyl carbon and nitrogen atoms.

The Oxford Diffraction software CrysAlisCCD and CrysAlisRED programs were used during the data collection, cell refinement and data reduction processes [20]. The SHELX-97 program [21] was used for the structure solution and refinement. The structure drawings were prepared using SHELXTL program [19].

The crystal data and the structure determination details for $[(CH_3)_3NH]_3[Sb_2Cl_9]$ at 165 and 95 K are listed in Table 1. The final atomic coordinates and equivalent isotropic displacement parameters for non-hydrogen atoms are shown in Table 2. The bond lengths, angles and the hydrogen bonds are presented in Tables 3 and 4, respectively.

Table 1
Crystal data, X-ray measurements and structure determination summary for $[(CH_3)_3NH]_3[Sb_2Cl_9]$ at 165 and 95 K

	165 K	95 K
Empirical formula	$C_9H_{30}Cl_9N_3Sb_2$	
Formula weight	742.91	
Crystal color; habit	Colorless; hexagonal-shaped plates	
Crystal size (mm^3)	$0.23 \times 0.22 \times 0.15$	
Crystal system	Monoclinic	
Space group	*Pc*	
Unit cell dimensions (Å, °)	$a = 9.9612(11)$	$a = 9.9138(10)$
	$b = 9.0714(8)$	$b = 9.0783(7)$
	$c = 15.1807(14)$	$c = 15.1299(14)$
	$\beta = 90.086(8)$	$\beta = 90.026(8)$
Volume ($Å^3$)	1371.8(2)	1361.7(2)
Z	2	
Density (calculated) ($g\,cm^{-3}$)	1.799	1.812
Wavelength (Å)	Mo$K\alpha$, $\lambda = 0.71073$	
Absorption coefficient (mm^{-1})	2.846	2.867
F(000)	720	
θ Range (°)	4.67–32.00	4.69–31.99
Index ranges	$-14 \leqslant h \leqslant 14$; $-13 \leqslant k \leqslant 13$; $-22 \leqslant l \leqslant 22$	$-14 \leqslant h \leqslant 14$; $-13 \leqslant k \leqslant 13$; $-22 \leqslant l \leqslant 22$
Reflections collected/unique	46400/8550 ($R_{int} = 0.0250$)	46002/8460 ($R_{int} = 0.0234$)
Observed reflections [$I > 2\sigma(I)$]	7578	7915
Data/parameters	8550/217	8460/217
Goodness of fit on F^2	1.108	1.173
Final *R* indices [$I > 2\sigma(I)$]	$R_1 = 0.0202$, w$R_2 = 0.0405$	$R_1 = 0.0163$, w$R_2 = 0.0356$
R Indices (all data)	$R_1 = 0.0254$, w$R_2 = 0.0486$	$R_1 = 0.0197$, w$R_2 = 0.0534$
Absolute structure parameter	0.030(11)	−0.017(12)
Largest diff. peak and hole ($e\,Å^{-3}$)	1.245 and −0.838	0.873 and −0.823

Crystallographic data (excluding structure factors) for tris(trimethylammonium) nonachlorodiantimonate(III) at 165 and 95 K have been deposited at the Cambridge Crystallographic Data Centre as supplementary publication nos. CCDC 235773 and 235774, respectively. Copies of the data can be obtained, free of charge, on application to the Director, CCDC, 12 Union Road, Cambridge CB2 1EZ, UK (Fax: int. code + (1223) 336033; e-mail: deposit@ccdc.cam.ac.uk or http://www.ccdc.cam.ac.uk).

3. Results and discussion

3.1. Synthesis of chloroantimonates(III) with selected organic cations

The ratio of monoprotonated organic cations to antimony(III)/bismuth(III) atoms in the structures of halogenoantimonates(III) and halogenobismuthates(III) varies from 1/3 to 4/1 [2,22]. This leads to the formation of a great variety of anionic sublattices differing in charges, sizes, shapes and properties. Since no systematic theory yet exists to predict the formula and the phase transition behavior of a given compound that is characterized, we decided to undertake the systematic study of the influence of molar ratio of substrates used in the reaction on the formula and properties of chloroantimonates(III).

The investigations were performed in a relatively wide range of molar ratios of organic cation to the antimony(III) atom, from 0.1:1 to 10:1. The changes of the molar ratios were carried out at least in every single unit in the range from 1:1 to 10:1, and every 0.2–0.3 units in the range from 0.1:1 to 1:1. Chloroantimonates(III) were investigated with: $(CH_3NH_3)^+$ methyl-, $[(CH_3)_2NH_2]^+$ dimethyl-, $[(CH_3)_3NH]^+$ trimethyl-, $[(CH_3)_4N]^+$ tetramethyl-, $(C_2H_5NH_3)^+$ ethylammonium, $[NH_3(CH_2)_2NH_3]^{2+}$ ethylene- and $[(CH_3)_2NH(CH_2)_2NH_3]^{2+}$ *N*,*N*-dimethylethylenediammonium as well as $[NH_2C(N(CH_3)_2)_2]^+$ N, N, N', N'-tetramethylguanidinium cations.

Fig. 1 presents the results of investigations. The pattern of each rectangle corresponds to the appropriate general formula (given at the bottom) of chloroantimonate(III) with organic cation. The blank places in rectangles, usually at the edges in the vicinity of ca. 0.2 and 8.5, mean that in these ranges the salts have not been obtained or that it crystallized the substrate (e.g., hydrochloride of amine) of the reaction.

It should be emphasized that the border point between two different crystallized salts cannot be determined precisely. There was usually a range, including one or two units, in which crystals of two different formulas were presented. In Fig. 1 the border

Table 2
Atomic coordinates (10^4) and equivalent isotropic displacement parameters (Å^2, 10^3) for non-hydrogen atoms of $[(CH_3)_3NH]_3[Sb_2Cl_9]$ at 165 and 95 K

Atom	x	y	z	U_{eq}
165 K				
Sb1	1(1)	2056(1)	0(1)	19(1)
Sb2	3028(1)	7092(1)	1719(1)	19(1)
Cl1	−1156(1)	133(1)	−773(1)	28(1)
Cl2	−1226(1)	1493(1)	1320(1)	28(1)
Cl3	−1792(1)	3825(1)	−405(1)	30(1)
Cl4	1501(1)	4416(1)	1206(1)	35(1)
Cl5	1126(1)	2805(1)	−1873(1)	31(1)
Cl6	1849(1)	−166(1)	542(1)	31(1)
Cl11	4274(1)	9117(1)	2384(1)	31(1)
Cl12	4775(1)	6730(1)	594(1)	31(1)
Cl13	4220(1)	5391(1)	2645(1)	29(1)
N1A	−1465(2)	3141(2)	−3102(2)	26(1)
C1A	−2116(4)	4615(3)	−3089(2)	37(1)
C2A	−2343(4)	2036(3)	−2684(2)	41(1)
C3A	−1112(4)	2706(4)	−4009(3)	40(1)
N2A	4504(2)	1696(3)	340(2)	27(1)
C4A	5459(4)	599(4)	−19(3)	47(1)
C5A	5073(4)	2466(4)	1115(2)	38(1)
C6A	4107(4)	2761(4)	−345(2)	43(1)
N3B	1498(3)	3186(3)	3261(2)	35(1)
C7B	26(4)	3272(4)	3348(3)	45(1)
C8B	1906(5)	1742(4)	2926(3)	57(1)
C9B	2150(5)	3565(5)	4106(2)	65(1)
95 K				
Sb1	4(1)	2042(1)	1(1)	12(1)
Sb2	3025(1)	7090(1)	1717(1)	12(1)
Cl1	−1147(1)	124(1)	−784(1)	17(1)
Cl2	−1225(1)	1460(1)	1328(1)	17(1)
Cl3	−1812(1)	3805(1)	−398(1)	18(1)
Cl4	1494(1)	4406(1)	1212(1)	21(1)
Cl5	1119(1)	2818(1)	−1875(1)	19(1)
Cl6	1851(1)	−175(1)	540(1)	19(1)
Cl11	4262(1)	9119(1)	2391(1)	19(1)
Cl12	4797(1)	6724(1)	592(1)	19(1)
Cl13	4220(1)	5396(1)	2654(1)	18(1)
N1A	−1473(3)	3168(3)	−3114(2)	17(1)
C1A	−2136(3)	4637(3)	−3101(2)	22(1)
C2A	−2339(4)	2048(3)	−2686(2)	26(1)
C3A	−1112(4)	2720(4)	−4033(2)	24(1)
N2A	4509(3)	1699(3)	355(2)	17(1)
C4A	5467(4)	587(4)	2(3)	29(1)
C5A	5083(4)	2479(4)	1129(2)	23(1)
C6A	4112(4)	2759(4)	−343(2)	26(1)
N3B	1490(3)	3222(3)	3262(2)	20(1)
C7B	8(3)	3299(4)	3344(2)	27(1)
C8B	1935(4)	1761(4)	2936(3)	32(1)
C9B	2140(4)	3597(4)	4118(2)	35(1)

U_{eq} is defined as one third of the trace of the orthogonalized U_{ij} tensor.

Table 3
Selected bond lengths (Å) and angles (°) for $[(CH_3)_3NH]_3[Sb_2Cl_9]$ at 165 K and 95 K

Atoms	165 K	95 K
Sb1–Cl1	2.3960(7)	2.3966(7)
Sb1–Cl2	2.4036(8)	2.4081(8)
Sb1–Cl3	2.4776(7)	2.4830(7)
Sb1–Cl4	3.1874(8)	3.1847(8)
Sb1–Cl5	3.1320(8)	3.1265(8)
Sb1–Cl6	2.8502(8)	2.8400(7)
Sb2–Cl11	2.4350(7)	2.4359(7)
Sb2–Cl12	2.4616(8)	2.4693(8)
Sb2–Cl13	2.4006(7)	2.4028(7)
Sb2–Cl4	2.9685(8)	2.9703(7)
Sb2–Cl5^{I}	2.8605(9)	2.8497(8)
Sb2–Cl6^{II}	3.2789(8)	3.2703(8)
Cl1–Sb1–Cl2	90.51(3)	90.71(3)
Cl1–Sb1–Cl3	90.23(3)	90.16(2)
Cl1–Sb1–Cl4	174.14(2)	174.47(2)
Cl1–Sb1–Cl5	83.45(3)	83.25(2)
Cl1–Sb1–Cl6	86.37(2)	86.22(2)
Cl2–Sb1–Cl3	88.70(3)	88.66(3)
Cl2–Sb1–Cl4	84.40(2)	84.44(2)
Cl2–Sb1–Cl5	170.38(2)	170.26(2)
Cl2–Sb1–Cl6	86.44(3)	86.07(2)
Cl3–Sb1–Cl4	92.56(2)	92.38(2)
Cl3–Sb1–Cl5	83.85(2)	83.74(2)
Cl3–Sb1–Cl6	174.04(3)	173.56(3)
Cl4–Sb1–Cl5	101.97(2)	101.91(2)
Cl4–Sb1–Cl6	90.40(2)	90.78(2)
Cl5–Sb1–Cl6	100.60(2)	101.08(2)
Cl11–Sb2–Cl12	91.61(3)	91.85(3)
Cl11–Sb2–Cl13	89.45(3)	89.40(3)
Cl11–Sb2–Cl4	170.52(3)	170.05(2)
Cl11–Sb2–Cl5^{I}	90.17(3)	89.94(3)
Cl11–Sb2–Cl6^{II}	80.55(2)	80.37(2)
Cl12–Sb2–Cl13	88.34(3)	88.30(3)
Cl12–Sb2–Cl4	94.09(3)	94.35(2)
Cl12–Sb2–Cl5^{I}	172.97(2)	172.59(2)
Cl12–Sb2–Cl6^{II}	88.65(2)	88.83(2)
Cl13–Sb2–Cl4	83.16(3)	83.02(2)
Cl13–Sb2–Cl5^{I}	84.87(3)	84.53(3)
Cl13–Sb2–Cl6^{II}	169.47(2)	169.28(2)
Cl4–Sb2–Cl5^{I}	83.28(2)	82.96(2)
Cl4–Sb2–Cl6^{II}	107.12(2)	107.50(2)
Cl5^{I}–Sb2–Cl6^{II}	98.35(2)	98.56(2)
Sb1–Cl4–Sb2	160.00(3)	159.66(3)
Sb1–Cl5–Sb2^{III}	157.49(3)	156.92(3)
Sb1–Cl6–Sb2^{IV}	157.59(3)	157.50(3)

Symmetry codes: (^{I}) x, $-y+1$, $z+1/2$; (^{II}) x, $y+1$, z; (^{III}) x, $-y+1$, $z-1/2$; (^{IV}) x, $y-1$, z.

point is in the center of the range, where two different crystals were obtained. The above-mentioned situation takes, among other things, place in the case of salts with the $(CH_3NH_3)^+$ methylammonium cation. In the molar ratio of methylamine to antimony(III) from 0.1:1 to 5:1 crystals of the $R_3Sb_2Cl_9$ formula were obtained. When the molar ratio increased to the 6:1–7:1 range, the two different crystals of $R_3Sb_2Cl_9$ and R_3SbCl_6 formulas were crystallized. The renewed increasing of molar ratio leads to the crystallization of salts of the R_3SbCl_6 formula. The border point between salts of the $R_3Sb_2Cl_9$ and R_3SbCl_6 formulas was assumed at the molar ratio of 6.5:1.

The investigations have undoubtedly proved that the formula of obtained salts is not completely accidental. With increasing the molar ratio of an organic cation to

the antimony(III) atom the ratio of these components also increases in the crystallized products. In the case of salts with dimethylammonium cation in the 0.6:1–5.5:1 range the salt of $R_3Sb_2Cl_9$ formula was obtained (R:Sb = 1.5:1). Increasing the molar ratio of substrates to 5.5:1–9.5:1 leads to crystallization of the R_2SbCl_5 salt (R:Sb = 2:1). Additional increase in the range between 9.5:1 and 10:1 results in crystallization of the R_4SbCl_7 salt (R:Sb = 4:1). A similar situation was also found in other studied chloroantimonates(III) (Fig. 1).

The reaction, in the same experimental conditions, between antimony(III) chloride and amines of the same size, chemical composition and geometry of their molecules—ethylamine and dimethylamine leads to the crystallization of different salts. Crystals of the $R_3Sb_2Cl_9$, R_2SbCl_5 and R_4SbCl_7 formulas were obtained in the reaction of dimethylamine and antimony(III) chloride, whereas when we used the same antimony(III) chloride and ethylamine we obtained $R_4Sb_3Cl_{13}$ and R_3SbCl_6 salts. However, when we check precisely the structure of the anionic sublattices and properties of mentioned dimethyl- and ethylammonium chloroantimonates(III) we find some similarities. The general formula of the $R_4Sb_3Cl_{13}$ salt could be, taking into account the structure of its anionic sublattice, considered as $R_3Sb_2Cl_9 \cdot RSbCl_4$ and salt of the R_3SbCl_6 formula could be written as $R_2SbCl_5 \cdot RCl$. They correspond well to those found in dimethylammonium chloroantimonates(III). Additionally, in the case of the $R_3Sb_2Cl_9 \cdot RSbCl_4$ salt with ethylammonium cation, similarly to the $R_3Sb_2Cl_9$ crystal with dimethylammonium one, the phase transition was found.

Most of obtained crystals are characterized by the $R_3Sb_2Cl_9$ formula. The preference in crystallization of salts of this stoichiometry, as some authors have suggested, is a function of their solubility [7]. Among obtained salts of the $R_3Sb_2Cl_9$ formula most possess anionic sublattices built of the $[\{Sb_2Cl_9\}_n]^{3n-}$ polyanionic layers composed of the corner-sharing $[SbCl_6]^{3-}$ octahedra. Taking into account obtained results the formation of this important, from the point of view of potential technical applications, type of sublattices of $R_3Sb_2Cl_9$ salts seems to be determined by the dimensions of the organic cations. The $R_3Sb_2Cl_9$ methylammonium chloroantimonate(III) crystal is characterized by the anionic sublattice composed of one-dimensional double zig-zag chain. The dimethyl- and trimethylammonium salts possess the layered sublattices, whereas in the tetramethylammonium one the isolated bioctahedral units are presented [5,23–25].

It should be noted, especially in the case of larger in spatial dimensions organic cations, that irrespective of the molar ratio of reactants, mainly one or only one salt was crystallized. The similar situation—formation of only one type of salt was reported, e.g., for the reaction of cyclohexylamine and antimony(III) bromide [26]. On

Table 4
Hydrogen bond geometries (Å, °) for $[(CH_3)_3NH]_3[Sb_2Cl_9]$ at 165 and 95 K

D–H···A	D–H	H···A	D···A	D–H···A
165 K				
N1A–H1A···Cl5	0.90	2.31	3.197(2)	167.0
N2A–H11A···Cl6	0.90	2.28	3.154(3)	163.6
N3B–H1B···Cl4	0.90	2.58	3.313(3)	139.5
N3B–H1B···Cl13	0.90	2.84	3.497(3)	130.9
C2A–H6A···Cl11^{I}	0.96	2.79	3.530(4)	134.2
C7B–H3B···Cl1^{II}	0.96	2.71	3.565(4)	148.2
C7B–H4B···Cl2	0.96	2.76	3.691(4)	163.4
95 K				
N1A–H1A···Cl5	0.90	2.32	3.196(2)	165.1
N2A–H11A···Cl6	0.90	2.28	3.149(3)	161.9
N3B–H1B···Cl4	0.90	2.55	3.283(3)	138.7
N3B–H1B···Cl13	0.90	2.82	3.473(3)	130.8
C2A–H6A···Cl11^{I}	0.96	2.80	3.534(4)	134.3
C7B–H3B···Cl1^{II}	0.96	2.70	3.565(4)	149.8
C7B–H4B···Cl2	0.96	2.77	3.685(4)	160.6

Symmetry codes: (^{I}) $x-1, -y+1, z-1/2$; (^{II}) $x, -y, z+1/2$.

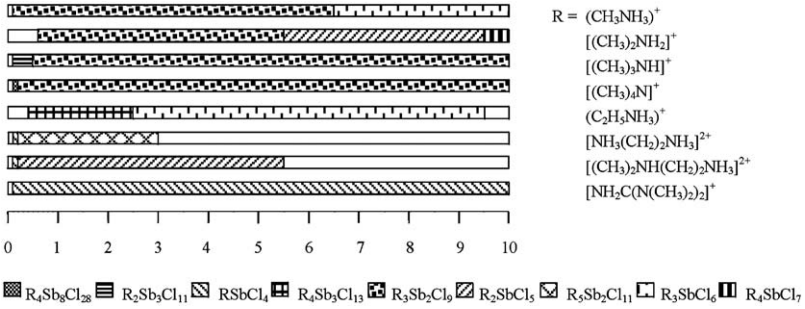

Fig. 1. The dependence of molar ratio of substrates on the general formula of crystallized chloroantimonates(III) with R (considered as monoprotonated) organic cations: $(CH_3NH_3)^+$ methyl-, $[(CH_3)_2NH_2]^+$ dimethyl-, $[(CH_3)_3NH]^+$ trimethyl-, $[(CH_3)_4N]^+$ tetramethyl-, $(C_2H_5NH_3)^+$ ethylammonium, $[NH_3(CH_2)_2NH_3]^{2+}$ ethylene-, and $[(CH_3)_2NH(CH_2)_2NH_3]^{2+}$ N,N-dimethylethylenediammonium as well as $[NH_2C(N(CH_3)_2)_2]^+$ N,N,N',N'-tetramethylguanidinium one. The pattern of each rectangle corresponds to the general formula of chloroantimoante(III) with organic cation. The axis gives molar ratio of substrates, organic cation to antimony(III) atom, e.g., number '1' means that the molar ratio of substrates is 1:1, '4' that it is 4:1.

the basis of formulas of obtained chloroantimonates(III), and analogous bromoantimonates(III) [7], we may assume that following equilibria exist in an aqueous HCl containing amine (amine hydrochloride) and antimony(III) chloride:

$$SbCl_3 + Cl^- \rightleftharpoons [SbCl_4]^-$$

$$2[SbCl_4]^- + Cl^- \rightleftharpoons [Sb_2Cl_9]^{3-}$$

$$[SbCl_4]^- + Cl^- \rightleftharpoons [SbCl_5]^{2-}$$

$$[SbCl_5]^{2-} + Cl^- \rightleftharpoons [SbCl_6]^{3-}$$

$$2[SbCl_5]^{2-} + Cl^- \rightleftharpoons [Sb_2Cl_{11}]^{5-}$$

Therefore, as was concluded by Jha and Rizvi [7], it is very difficult to predict the formulas of these crystals. The same authors suggested that crystallization of the last soluble salt for each organic cation is preferred. It seems, that in this way, it could be explained that the distinctness of N,N,N',N'-tetramethylguanidinium chloroantimonate(III)—the only one salt with a different formula from $R_3Sb_2Cl_9$ was obtained.

The ethylene- and *N*,*N*-dimethylethylenediammonium cations are distinguished by their structures. They possess two independent, NH_3^+ (NH^+) groups, which are potentially capable of forming simultaneously N–H $\cdots$ Cl hydrogen bonds. The reaction of antimony(III) chloride, with these organic substances, leads to the formation of three different $RSbCl_4$, $R_5Sb_2Cl_{11}\cdot 4H_2O$ and R_2SbCl_5 salts. The first one, in the case of both organic cations, crystallizes in a relatively narrow range of the molar ratios. It should be mentioned that above the molar ratio of 3:1 and 5.5:1 crystallizes only the substrate of the reaction—ethylenediammonium dichloride or it does not crystallize any product in the case of ethylediammonium and *N*,*N*-dimethylethylenediammonium cations, respectively.

To sum up, the studied chloroantimonates(III) with different organic cations crystallize in the relatively wide range of molar ratios of substrates. The average molar ratio of crystallized salts is between 0.2:1 and 8.5:1. The same products are obtained in the wide range of molar ratio, in some cases significantly different from the theoretical one, e.g., the $R_3Sb_2Cl_9$ salt is obtained in the molar ratio from 0.1:1 to 10:1, but the theoretical one is 1.5:1. During the reaction of two substrates at least one product could be crystallized. Using the same substrates, changing only their molar ratio, a maximum of three different products were obtained. In all cases the crystallization of one, in some cases only one product, is preferred. The remaining products for given substrates are obtained in the relatively narrow range of molar ratios.

3.2. Crystal structures of $[(CH_3)_3NH]_3[Sb_2Cl_9]$ at 165 and 95 K

Tris(trimethylammonium) nonachlorodiantimonate(III), $[(CH_3)_3NH]_3[Sb_2Cl_9]$, taking into account its polar properties, is one of the most interesting chloroantimonate(III). The crystal is characterized by one of the highest value of spontaneous polarization (ca. $3\,10^{-2}\,C\,m^{-2}$) in the whole family of halogenoantimonates(III) and halogenobismuthates(III) with organic cations. Additionally, it exhibits ferroelectricity in a wide temperature range, between 363 and 13 K.

The structure of $[(CH_3)_3NH]_3[Sb_2Cl_9]$ was determined at 165 and 95 K, below the low-temperature phase transitions reported at 203 and 125 K, respectively. The determined space group at both temperatures is monoclinic *Pc*. There are two crystallographically non-equivalent antimony(III) atoms in both structures. They are surrounded by nine independent chlorine ligands forming the $[SbCl_6]^{3-}$ distorted octahedra. The coordination sphere of each octahedron composes of three bridging and three terminal Cl atoms. At both temperatures the anionic sublattice of $[(CH_3)_3NH]_3[Sb_2Cl_9]$ is composed of, the above mentioned, $[SbCl_6]^{3-}$ octahedra that share *cis* corners, leading to the formation of characteristic six-membered $[Sb_6Cl_{27}]^{9-}$ rings, which finally are connected to each other forming polyanionic $[\{Sb_2Cl_9\}_n]^{3n-}$ layers in the *bc* plane of the crystal (Fig. 2). Two (N1A and N2A) out of three crystallographically independent $[(CH_3)_3NH]^+$ trimethylammonium cations are located between the

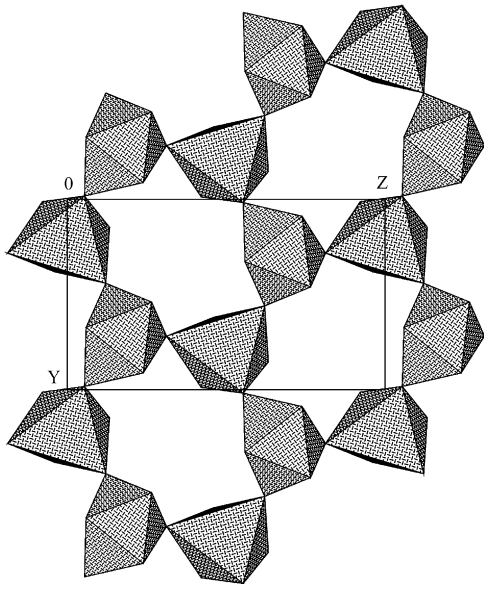

Fig. 2. The polyhedral representation of the polyanionic $[\{Sb_2Cl_9\}_n]^{3n-}$ layer built of characteristic six-membered $[Sb_6Cl_{27}]^{9-}$ rings in the structure of tris(trimethylammonium) nonachlorodiantimonate(III) at 95 K along the *a*-axis.

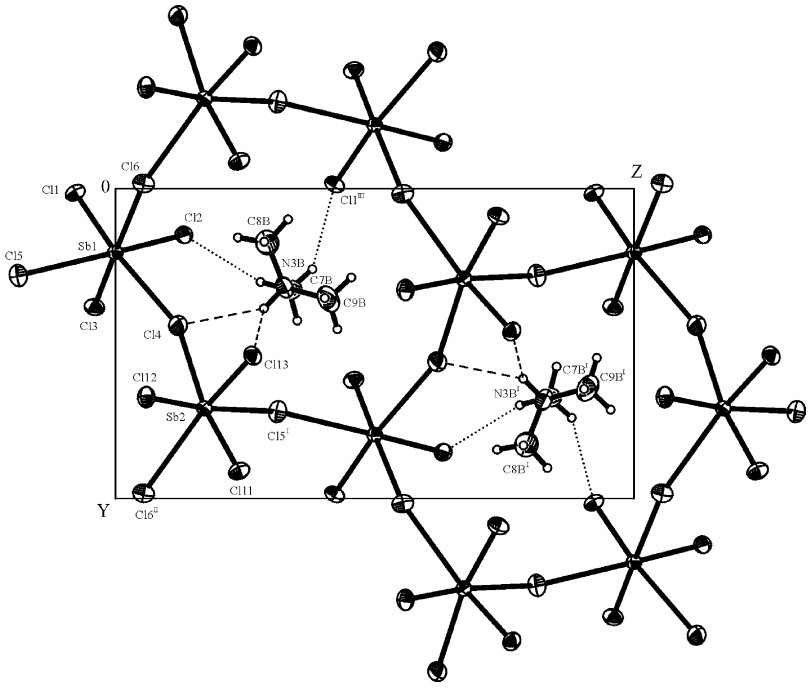

Fig. 3. The anionic sublattice with organic cations embedded inside the cavity formed by six $[SbCl_6]^{3-}$ octahedra in the structure of tris(trimethylammonium) nonachlorodiantimonate(III) at 165 K along the *a*-axis. The dashed lines indicate N–H···Cl, whereas dotted ones the C–H···Cl hydrogen bonds. Displacement ellipsoids are plotted at the 50% probability level. Symmetry codes: (I) $x, -y+1, z+1/2$; (II) $x, y+1, z$; (III) $x, -y, z+1/2$.

inorganic layers, whereas the third one (N3B) is embedded inside the six-membered ring (Fig. 3). In contrast to the structures of TMACA at 295 and 373 K, all cations at two studied temperatures were found to be ordered. The bond lengths and angles of the trimethylammonium cations at both temperatures are typical. They are similar to those found in other structures, e.g., [27].

The asymmetric parts of the unit cells and the labeling of atoms at both studied temperatures have been chosen to show the structural relationship between the positions of corresponding atoms at 95, 165 K, and in the previously reported structures at 295 and 373 K [16].

3.2.1. Structure at 165 K

In the structure of $[(CH_3)_3NH]_3[Sb_2Cl_9]$ the longest Sb–Cl bonds correspond to the bridging chlorine atoms and the shortest to the terminal, opposite to the bridging ones (*trans* influence [28,29]). The longest distances are 3.1874(8) and 3.2789(8) Å, while the shortest are 2.3960(7) and 2.4006(7) Å within the Sb1 and the Sb2 octahedra. The Cl–Sb–Cl angles involving chlorine atoms in the mutually *cis* range from 83.45(3)° to 101.97(2)°, and from 80.55(2)° to 107.12(2)°, while those *trans* located are between 170.38(2)° and 174.14(2)° for Sb1, and between 169.47(2)° and 172.97(2)° for the Sb2 octahedron. The Sb–Cl–Sb inter-octahedral angles range from 157.49(3)° to 160.00(3)° (Table 3).

The same anionic sublattice, built of octahedra connected by three corners, and finally forming polyanionic layers was, among other things, found in the structures of the same $[(CH_3)_3NH]_3[Sb_2Cl_9]$ crystal at 295 and 373 K [5,16,30], $[(CH_3)_2NH_2]_3[Sb_2Cl_9]$ (DMACA) at 200 and 298 K [24] and $[C(NH_2)_3][Sb_2Cl_9]$ (GNCA) at 298 K [31]. In all the structures the Sb–Cl bond lengths are in the same order—the longest are bridging, and the shortest terminal. The largest change, 0.916(4) Å, in Sb–Cl bond lengths within the same (Sb2) octahedron was found in the structure of the $[(CH_3)_3NH]_3[Sb_2Cl_9]$ salt at 295 K. Significant differences were also noticed in the case of *cis* Cl–Sb–Cl angles. The largest dissimilarity (because of the disordered Cl5 atom), 23.5(21)°, was noticed again in the structure of $[(CH_3)_3NH]_3[Sb_2Cl_9]$, but at 373 K.

It is also interesting to compare the deformation of the $[SbCl_6]^{3-}$ octahedra in the title structure with an isolated octahedron, not deformed by the formation of Sb–Cl–Sb bridges. Schroeder and Jacobson reported the structure of hexaamminecobalt hexachloroantimonate(III), $Co(NH_3)_6[SbCl_6]$, where the isolated $[SbCl_6]^{3-}$ octahedron was described [32]. All Sb–Cl distances are 2.643(6) Å (2.652(6) Å when corrected assuming a riding model), whereas the average Cl–Sb–Cl angle is 90.9(2)°. The average Sb–Cl bond lengths in TMACA for the Sb1 and the Sb2 octahedra are comparable 2.7411(8) and 2.7342(8) Å. They, on average, differ from the value

characteristic of the isolated reference octahedron by 0.086(7) Å.

The results described above clearly suggest that the deformation of inorganic layers in $[(CH_3)_3NH]_3[Sb_2Cl_9]$ is mainly related to bridging ligands. The largest difference, from the theoretical 90° and 180° in valence angles (22.51(3)°), was noticed for the inter-octahedral Sb–Cl–Sb angle. Additionally, the N–H···Cl and C–H···Cl hydrogen bonds between oppositely charged moieties also contribute to the deformation of the $[SbCl_6]^{3-}$ polyhedra (Figs. 3 and 4). The D···A distances are between 3.154(3) and 3.691(4) Å (Table 4). They are comparable to those found in other chloroantimonates(III) [24,33].

The literature explains that the distortions of the $[SbCl_6]^{3-}$ octahedra are mainly related to two reasons. (I) The tendency of $[SbCl_6]^{3-}$ octahedra to share bridging Cl atoms resulting in formation of polyanionic units, which is inseparable from the stereochemical activity of the 5*s* lone electron pair located on the Sb^{III} atom. The lone electron pair is assumed to occupy the spherical 5*s* orbital leaving the *p* and *d* orbitals to form octahedral hybrid [34,35]. (II) The presence of different in geometry and strength N···Cl and C···Cl interactions, which additionally move Cl atoms in the direction of organic cations, e.g., [24,36]. In our previously reported papers we have proved that these two phenomena, called the primary and secondary deformation, are responsible for the differences in the Sb–Cl bond lengths and Cl–Sb–Cl angles, e.g., [37].

In the structure of $[(CH_3)_3NH]_3[Sb_2Cl_9]$ the influence of hydrogen bonds is visible in the case of bridging Cl4, Cl5 and Cl6 atoms. Unfortunately, taking into account the D···A and H···A distances (the strongest N–H···Cl hydrogen bonds are formed to the bridging Cl atoms), it is rather difficult to separate and unambiguously determine the influence of the type of inorganic sublattice and, at the same time, the hydrogen bonds on the deformation of anionic layers.

3.2.2. Structure at 95 K

In the low-temperature phase of $[(CH_3)_3NH]_3[Sb_2Cl_9]$ the arrangement of the chloro ligands around the antimony(III) atoms similarly deviates from the ideal octahedral geometry as compared to the structure at 165 K. The Sb–Cl bond lengths are in the same order. The lengths of the Sb–Cl bonds vary from 2.3966(7) to 3.2703(8) Å. The largest difference between the shortest and the longest Sb–Cl distances is 0.8675(15) at 95 K and 0.8737(15) at 165 K, for the same Sb2 octahedron. In the case of the *cis* Cl–Sb–Cl angles the differences are 27.13(4)° and 26.57(4)° for the structure at 95 and 165 K, respectively (Table 3). In comparison with the Sb–Cl bond lengths and the Cl–Sb–Cl angles of the reference, isolated octahedron [32], the calculated deviations are, in general, somewhat smaller at 95 K than in the structure at 165 K.

The calculated octahedral distortion parameter Δ is a mean-square relative deviation from the average ($\Delta = 1/6\sum_{i=1}^{6}[(R_i - \bar{R})/\bar{R}]^2$, where $\bar{R}$ is the average bond length within octahedron and R_i the individual bond length of the octahedron) [38]. It clearly shows the distortions in the bond lengths of the octahedra, for two independent Sb1 and the Sb2 polyhedra in the structure of TMACA at 95 and 165 K. It is as much as: 0.01446, 0.01396, and 0.01478, 0.01433, respectively. The same parameter determined for the various AX_6E—systems (where *A*—central atom: Se, Te, Sb, Bi; *X*—ligand: Cl, Br I; *E*—unshared electron pair) is between 0.00 (for

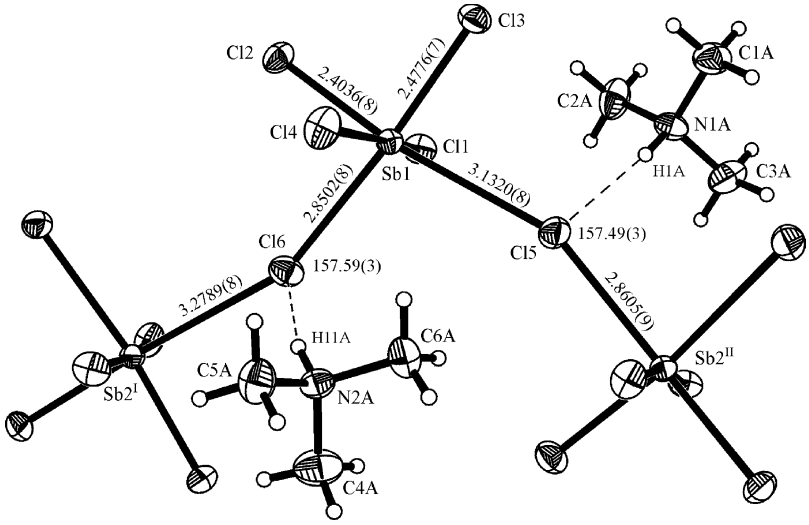

Fig. 4. The N–H···Cl hydrogen-bonding scheme (indicated by dashed lines) involving bridging Cl5 and Cl6 atoms in the structure of tris(trimethylammonium) nonachlorodiantimonate(III) at 165 K. Displacement ellipsoids are plotted at the 50% probability level. Symmetry codes: (I) $x, y-1, z$; (II) $x, -y+1, z-1/2$.

non-distorted systems) and 0.00835 (for $[DenH_3][SbCl_6]$, $DenH_3$—diethylenetriammonium cation) [39,40].

3.3. Phase transition in $[(CH_3)_3NH]_3[Sb_2Cl_9]$ at 125 K

The high- and low-temperature phase transitions, detected in $[(CH_3)_3NH]_3[Sb_2Cl_9]$ compound, have been the subject of several studies including, among others, calorimetric and spectroscopic measurements (NMR, IR, Raman) as well as dielectric and pyroelectric investigations [11,41–46]. Two closely lying high-temperature phase transitions, of the first and the second order, to the paraelectric phase were detected at 363 and 364 K, respectively. This ferroelectric-intermediate (incommensurate)-paraelectric phase transitions were also studied by the X-ray diffraction method [16,47]. The possibility of diffuse phase transition between two ferroelectric phases and the presence of continuous one between two polar phases, both of the second order, were reported at 203 and 125 K, respectively [42,46].

The previously reported X-ray investigations of $[(CH_3)_3NH]_3[Sb_2Cl_9]$ have shown that in the room-temperature ferroelectric phase two crystallographically independent trimethylammonium cations (N1A, N2A), located between the inorganic layers are ordered, whereas the third one (N3B), placed inside the inorganic $[Sb_6Cl_{27}]^{9-}$ ring, was found to be disordered [16].

The precise dielectric and pyroelectric studies of TMACA, also supported by previous investigations, suggested that at ca. 200 K the motions of the trimethylammonium cation (N3B) located inside the anionic layer are frozen [48]. The results of our X-ray diffraction studies, described above, prove that motions of the trimethylammonium cations embedded in $[\{Sb_2Cl_9\}_n]^{3n-}$ layers are gradually slowed down with decreasing temperature. At 165 K all organic cations are ordered. The process of the ordering of the N3B trimethylammonium cation, located in the general position, do not lead to the phase transition and is considered as a next step in the process of its freezing. It should be stressed that owing the ordering of the N3B trimethylammonium cation, the N–H$\cdots$Cl hydrogen bonds involving this cation are somewhat stronger, particularly in the case of the N3B$\cdots$Cl4 interactions, at 165 K than at 295 K.

The mechanism of the phase transition at 125 K, based on the dielectric and pyroelectric anomalies, was concluded to be the continuous structural transformation between two polar phases, related to the motion of the $-CH_3$ methyl groups of organic cations [48]. According to the described above X-ray results, it could be considered as a non-structural transition related to the subtle structural effects and changes in the molecular dynamics of organic cations or as, which is less probable, the structural isomorphous phase transition. In our opinion the mechanism of this phase transition should be interpreted as a further step in freezing of motions of the cationic sublattice, which do not lead to the structural phase transition. The observed decrease in thermal motions, reflected in the relatively low displacement parameters of C and N atoms of trimethylammonium cations in the low-temperature phase as compared to the room-temperature one, together with rather insignificant changes in the hydrogen-bonding schemes clearly suggests, that reorientations of this ion were slowed down. The process is mainly related not only with changes in strength of hydrogen bonds but also with an interaction of cations with their environment as a whole.

The additional experimental information is needed to go further in the study of the phase transition occurring in the TMACA crystal in the low-temperature region. In particular the suggested non-structural character of the transition at 125 K has to be confirmed.

The determination of crystal structures of the $[(CH_3)_3NH]_3[Sb_2Cl_9]$ salt confirms another interesting phenomenon found during the studies of ferroelectric properties of halogenoantimonates(III) and halogenobismuthates(III) with organic cations. Bator et al. and Wojtaś et al. investigated the mixed $[(CH_3)_3NH]_3[Sb_{2(1-x)}Bi_{2x}Cl_9]$ ($x = 0$, 0.07, 0.33, 0.38 and 1) and $[(CH_3)_3NH]_3[Sb_2Cl_{9(1-x)}Br_{9x}]$ ($x = 0$, 0.02, 0.17 and 0.42) crystals containing trimethylammonium cation. The studies clearly showed that the gradual replacement of Sb or Cl atoms with larger Bi or Br ones leads to the deformation and finally to the change (Bi atom concentration above $x = 0.33$ or Br atom above ca. 60%) of the layered $[\{M_2X_9\}_n]^{3n-}$ sublattice to the isolated bioctahedral $[M_2X_9]^{3-}$ units. At the same time the destruction of the polyanionic sublattice the high electric polarizability disappears [49,50].

4. Conclusions

The studied chloroantimonates(III) with selected organic cations were obtained in the relatively wide range of molar ratios of substrates. There are preferences in crystallization of one, in some cases the only one, product in the reaction of antimony(III) chloride and an organic substance. The changes of the molar ratio of substrates reflect the corresponding changes of organic and inorganic components in the crystallized salts. Although we are not able to predict exactly how many and which products are possible to obtain, we can satisfactory plan and assume the sequence of the crystallizing salts and in a consequence eliminate the impossible ones.

The structure of $[(CH_3)_3NH]_3[Sb_2Cl_9]$ salt was investigated at 165 and 95 K using the single-crystal X-ray diffraction method. At both temperatures, the polar *Pc* space group, the structure is built of polyanionic

Table 5
Phase behavior in $[(CH_3)_3NH]_3[Sb_2Cl_9]$

Temperature of phase transition (K)		125 (?)		363	364
Nature of phase transition		Ferro–ferroelectric		Para–ferroelectric Incommensurate	Structural
Order of phase transition		Second		First	Second
Temperature of X-ray investigations (K)	95	165	295		373
Space group		Pc	Pc		$P2_1/c$
Number of all/disordered $[(CH_3)_3NH]^+$ cations		3/0	3/1		2/2

$[\{Sb_2Cl_9\}_n]^{3n-}$ layers and $[(CH_3)_3NH]^+$ cations. The interionic interactions as well as hydrogen bonds have the strong influence on the deformation of the basic inorganic building blocks—$[SbCl_6]^{3-}$ octahedra, especially in the case of the geometrical parameters related to the bridging, the farthest from the central atom located, ligands. The crystals of $[(CH_3)_3NH]_3[Sb_2Cl_9]$ may undergo one low-temperature phase transition 125 K. The mechanism of this non-structural transition is mainly associated with the slowing down of reorientations of the trimethylammonium cations. The phase behavior in $[(CH_3)_3NH]_3[Sb_2Cl_9]$ including the most important information characterizing each phase is depicted in Table 5.

References

[1] R. Jakubas, L. Sobczyk, Phase Trans. 20 (1990) 163.
[2] G.A. Fischer, N.C. Norman, Adv. Inorg. Chem. 41 (1994) 233.
[3] L. Sobczyk, R. Jakubas, J. Zaleski, Polish J. Chem. 71 (1997) 265.
[4] R. Jakubas, G. Bator, Z. Ciunik, Ferroelectrics 295 (2003) 3.
[5] F.J. Kruger, F. Zettler, A. Schmidt, Z. Anorg. Allg. Chem. 449 (1979) 135.
[6] U. Ensinger, W. Schwarz, A. Schmidt, Z. Naturforsch. 37b (1982) 1584.
[7] N.K. Jha, S.S.A. Rizvi, J. Inorg. Nucl. Chem. 38 (1976) 401.
[8] R.D. Whealy, J.B. Blackstock Jr., J. Inorg. Nucl. Chem. 26 (1964) 243.
[9] R. Jakubas, Z. Galewski, L. Sobczyk, J. Matuszewski, J. Phys. C 18 (1985) L857.
[10] R. Jakubas, Solid State Commun. 60 (1986) 389.
[11] R. Jakubas, Z. Czapla, Z. Galewski, L. Sobczyk, Ferroelectrics Lett. 5 (1986) 143.
[12] R. Jakubas, Solid State Commun. 69 (1989) 267.
[13] R. Jakubas, Z. Ciunik, G. Bator, Phys. Rev. B 67 (2003) 024103–1.
[14] M. Bujak, Ph.D. Thesis, University of Opole, Opole, Poland 2000.
[15] M. Bujak, P. Osadczuk, J. Zaleski, Acta Crystallogr. C 57 (2001) 388.
[16] M. Bujak, J. Zaleski, Cryst. Eng. 4 (2001) 241.
[17] M. Bujak, J. Zaleski, Z. Naturforsch. 56b (2001) 521.
[18] M. Bujak, J. Zaleski, Main Group Met. Chem. 25 (2002) 571.
[19] G.M. Sheldrick, SHELXTL, Siemens Analytical X-ray Instrument Inc., Madison, Winsconsin, USA, 1990.
[20] Oxford Diffraction; CrysAlis CCD, Data collection GUI for CCD and CrysAlis RED, CCD data reduction GUI versions 1.169.5 and 1.170.16, Oxford Diffraction, Poland, 2002.
[21] G.M. Sheldrick, SHELX-97. Program for the Solution and the Refinement of Crystal Structures, University of Göttingen, Germany, 1997.
[22] J. Zaleski, Structure, Phase Transitions and Molecular Motions in Chloroantimonates(III) and Bismuthates(III), Opole University Press, Opole, Poland, 1995.
[23] R. Jakubas, Z. Czapla, Z. Galewski, L. Sobczyk, O.J. Żogał, T. Lis, Phys. Stat. Sol. (a) 93 (1986) 449.
[24] J. Zaleski, A. Pietraszko, Acta Crystallogr. B 52 (1996) 287.
[25] H. Ishihara, K. Watanabe, A. Iwata, Y. Yamada, Y. Kinoshita, T. Okuda, V.G. Krishnan, S. Dou, A.Z. Weiss, Z. Naturforsch. 47a (1992) 65.
[26] R.D. Whealy, R.L. Yeakley, J. Inorg. Nucl. Chem. 25 (1963) 365.
[27] G. Thiele, G. Wittenburg, Acta Crystallogr. C 54 (1998) 764.
[28] G.A. Landrum, R. Hoffmann, Angew. Chem. Int. Ed. 37 (1998) 1887.
[29] K.M. Anderson, A.G. Orpen, Chem. Commun. (2001) 2682.
[30] A. Kallel, J.W. Bats, Acta Crystallogr. C 41 (1985) 1022.
[31] J. Zaleski, to be published.
[32] D.R. Schroeder, R.A. Jacobson, Inorg. Chem. 12 (1973) 210.
[33] M. Bujak, J. Zaleski, J. Chem. Crystallogr. 29 (1999) 555.
[34] R.J. Gillespie, Chem. Soc. Rev. (1992) 59.
[35] X. Wang, F. Liebau, Acta Crystallogr. B 52 (1996) 7.
[36] M. Bujak, J. Zaleski, Acta Crystllogr. C 54 (1998) 1773.
[37] M. Bujak, J. Zaleski, Z. Naturforsch. 57b (2002) 157.
[38] I.D. Brown, R.D. Shannon, Acta Crystallogr. A 29 (1973) 266.
[39] W. Abriel, Z. Naturforsch. 42b (1987) 415.
[38] I.D. Brown, R.D. Shannon, Acta Crystallogr. A 29 (1973) 266.
[39] W. Abriel, Z. Naturforsch. 42b (1987) 415.
[40] A. du Bois, W. Abriel, Z. Naturforsch. 43b (1988) 1003.
[41] R. Jakubas, A. Miniewicz, M. Bertault, J. Sworakowski, A. Collet, J. Phys. France 50 (1989) 1483.
[42] S. Idziak, R. Jakubas, Solid State Commun. 62 (1987) 173.
[43] B. Jagadeesh, P.K. Rajan, K. Venu, V.S.S. Sastry, Solid State Commun. 86 (1993) 803.
[44] A. Miniewicz, R. Jakubas, C. Ecolivet, A. Girard, J. Raman Spectrosc. 20 (1989) 381.
[45] V. Varma, R. Bhattacharjee, H.N. Vasan, C.N.R. Rao, Spectrochim. Acta 48A (1992) 1631.
[46] J. Mróz, Z. Czapla, R. Jakubas, Acta Phys. Pol. A70 (1986) 705.
[47] P.E. Tomaszewski, Acta Phys. Pol. A87 (1995) 631.
[48] G. Bator, R. Jakubas, L. Sobczyk, J. Mróz, Ferroelectrics 141 (1993) 177.
[49] G. Bator, R. Jakubas, J. Zaleski, J. Mróz, J. Appl. Phys. 88 (2000) 1015.
[50] M. Wojtaś, G. Bator, R. Jakubas, J. Zaleski, J. Phys.: Condens. Matter 15 (2003) 5765.